Tetrahedron Letters 53 (2012) 4580–4583

Contents lists available at SciVerse ScienceDirect

Tetrahedron Letters

journal homepage: www.elsevier.com/locate/tetlet

Synthesis and functional evaluation of chiral dendrimer–triamine-coordinated Gd complexes as highly sensitive MRI contrast agents

Yuka Miyake [a], Yu Kimura [b], Syungo Ishikawa [a], Hiroshi Tsujita [a], Hiroki Miura [a], Michiko Narazaki [c], Tetsuya Matsuda [c], Yasuhiko Tabata [d], Tetsuya Yano [e], Akio Toshimitsu [a,f], Teruyuki Kondo [a,b,*]

[a] Department of Energy and Hydrocarbon Chemistry, Graduate School of Engineering, Kyoto University, Nishikyo-ku, Kyoto 615-8510, Japan
[b] Advanced Biomedical Engineering Research Unit, Kyoto University, Nishikyo-ku, Kyoto 615-8510, Japan
[c] Graduate School of Informatics, Kyoto University, Yoshida-honmachi, Sakyo-ku, Kyoto 606-8501, Japan
[d] Institute for Frontier Medical Sciences, Kyoto University, 53 Kawaracho, Shogoin, Sakyo-ku 606-8507, Japan
[e] Canon Inc., 3-30-2 Shimomaruko, Ohta-ku, Tokyo 146-8501, Japan
[f] Institute for Chemical Research, Kyoto University, Gokasho, Uji, Kyoto 611-0011, Japan

ARTICLE INFO

Article history:
Received 24 April 2012
Revised 11 June 2012
Accepted 15 June 2012
Available online 20 June 2012

Keywords:
Chiral dendrimer
MRI contrast agent
Gadolinium
Drug design
Pharmacokinetics

ABSTRACT

Novel chiral dendrimer–triamine-coordinated Gd complexes were synthesized and shown to have longitudinal relaxivity ($r1$) 3 times higher than that of clinically used Gd-DTPA. The pharmacokinetic differences between optical isomers were estimated from the affinity of **2-(*R*)** and **2-(*S*)** with bovine serum albumin (BSA), respectively, by a quartz crystal microbalance (QCM) measurement. As a result, the association constant K_a of **2-(*S*)** was about 4 times higher than that of **2-(*R*)**, which means that **2-(*S*)** is retained in the vascular retention for a longer time after administration. This result was also supported by T1-weighted MR images of mice before and after the intravenous injection of **2-(*R*)** and **2-(*S*)**, as well as the time-course of the signal intensities (SI) at the blood vessels and quantification of Gd^{3+} concentration in the blood and urine.

Introduction

MRI has become a prominent non-invasive imaging technique for disease diagnosis.[1] Low-molecular-weight contrast agents based on Gd-DTPA (DTPA = diethylenetriaminepentaacetic acid) and Gd-DOTA (DOTA = 1,4,7,10-tetraazacyclododecane-1,4,7,10-tetraacetic acid) have been approved by the U.S. Food and Drug Administration (FDA) and the European Medicines Agency (EMEA), and are widely used in the clinical diagnosis of tumors (Fig. 1).[2]

However, the non-specificity, low contrast efficiency, and rapid renal excretion of these low-molecular-weight contrast agents necessitate a high dosage (ca. 0.5 M), which imposes a great physical strain on the patient, and in some cases they may produce side effects, such as osmotic pressure shock.[3] The main reason for their low contrast efficiency is that, among the nine coordination sites of Gd, up to eight are solidly occupied with ionic chelating ligands, and thus only one remains for coordination with free water molecules, which is observed by MRI (Fig. 1). In addition, the rotational motion of Gd metal in the center of existing small ligands cannot be suppressed, and as a result the image contrast is considerably reduced.

Therefore, there is a strong need for the development of highly sensitive MRI contrast agents, and recently there has been growing worldwide interest in the development of MRI contrast agents that consist of Gd-functionalized dendrimer macromolecules.[4] Dendrimers[5] are a unique category of macromolecules with well-controlled sizes, nanoscopic dimensions, and numerous peripheral chemical groups to which Gd chelates can be coupled. Gd-functionalized poly(amidoamine) (PAMAM)[6] and poly(propyleneimine) (PPI)[7] dendrimers have been reported and evaluated in animal models for high-resolution MRI, in which dendrimers were used as a core and Gd chelates were positioned in the periphery.[8] Unfortunately, among the Gd-functionalized dendrimers that have been reported for use as contrast agents, dendrimers were only

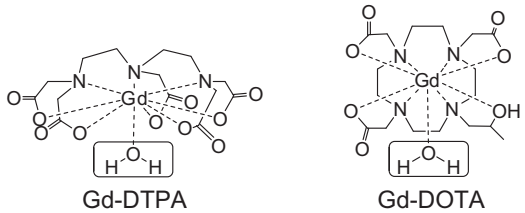

Figure 1. Structure of Gd-DTPA and Gd-DOTA.

* Corresponding author. Fax: +81 75 383 7055.
E-mail address: teruyuki@scl.kyoto-u.ac.jp (T. Kondo).

0040-4039/$ - see front matter © 2012 Elsevier Ltd. All rights reserved.
http://dx.doi.org/10.1016/j.tetlet.2012.06.072

used to slow the molecular tumbling and rotation of Gd. The intravascular retention time is prolonged, but the principle of reducing the ^{1}H relaxation time of a water molecule is the same as that with low-molecular-weight contrast agents.

In this study, we radically revised the concept of the established methods that use dendrimers, so that they could be used as a ligand at the periphery of a Gd metal. As a result, we succeeded in designing and synthesizing novel chiral dendrimer–triamine-coordinated Gd complexes which are expected to be highly sensitive MRI contrast agents.

Results and discussion

As shown in Scheme 1, **(*R*)-** and **(*S*)-**chiral diols, which serve as building blocks for chiral dendrimer–triamine ligands, were first prepared by the asymmetric dihydroxylation reaction developed by Sharpless and co-workers.[9] Repeated binding of these chiral diols gave the corresponding chiral dendrons in high yield and with high enantioselectivity.[10] Connection of the chiral dendrons to 1,4,7-triazacyclononane gave 2nd-generation chiral dendrimer–triamine ligands, in which all 9 of the stereogenic centers have an (*R*)- or (*S*)-configuration, respectively. Hydrolysis of the acetal protecting groups and complexation of $GdCl_3{\cdot}6H_2O$ gave novel chiral dendrimer–triamine-coordinated Gd complexes, **2-(*R*)** and **2-(*S*)**,[11] which are expected to be a highly sensitive MRI contrast agents.

Next, the longitudinal relaxivities (r1) of chiral dendrimer–triamine-coordinated Gd complexes (**2-(*R*)** and **2-(*S*)**), $GdCl_3{\cdot}6H_2O$, and Gd-DTPA were calculated in vitro (Fig. 2 and Table 1). The r1 values of **2-(*R*)** and **2-(*S*)** were 11.4 and 11.1 $mM^{-1}\,s^{-1}$, respectively, which are approximately 3 times higher than that of Gd-DTPA (r1 = 4.6 $mM^{-1}\,s^{-1}$).

As mentioned previously, the established low-molecular-weight Gd contrast agents such as Gd-DTPA and Gd-DOTA have ionic chelating ligands that strongly suppress 8 coordination sites of Gd. On the other hand, the novel Gd complexes have a triamine ligand and three chloride ligands, which stably occupy 6 coordination sites of Gd. Accordingly, 3 coordination sites remain for water molecules, and thus the present Gd complexes show longitudinal relaxivity that is 3 times higher than that of Gd-DTPA. In addition, the central Gd is considered to be covered through weak coordination by hydroxyl groups at the dendrimer end, and they may dissociate only when a small, but highly polar, water molecule approaches.[12] The binding (coordination) ability of 1,4,7-triazacyclononanes to Gd in **2-(*R*)** and **2-(*S*)** is considered to be high,[13] and no ligand-free Gd^{3+} was formed, which are strongly suggested by the following cytotoxicity examination.

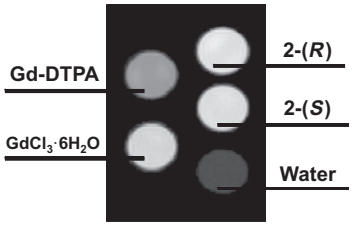

Figure 2. T1-weighted MR images of Gd-DTPA, $GdCl_3{\cdot}6H_2O$, **2-(*R*)**, **2-(*S*)** (0.50 mM) and water.

Table 1
Longitudinal relaxivities (r1) of Gd-DTPA, **2-(*R*)**, **2-(*S*)**, and $GdCl_3{\cdot}6H_2O$

Entry	r1/$mM^{-1}\,s^{-1}$
Gd-DTPA	4.6
2-(*R*)	11.4
2-(*S*)	11.1
$GdCl_3{\cdot}6H_2O$	14.6

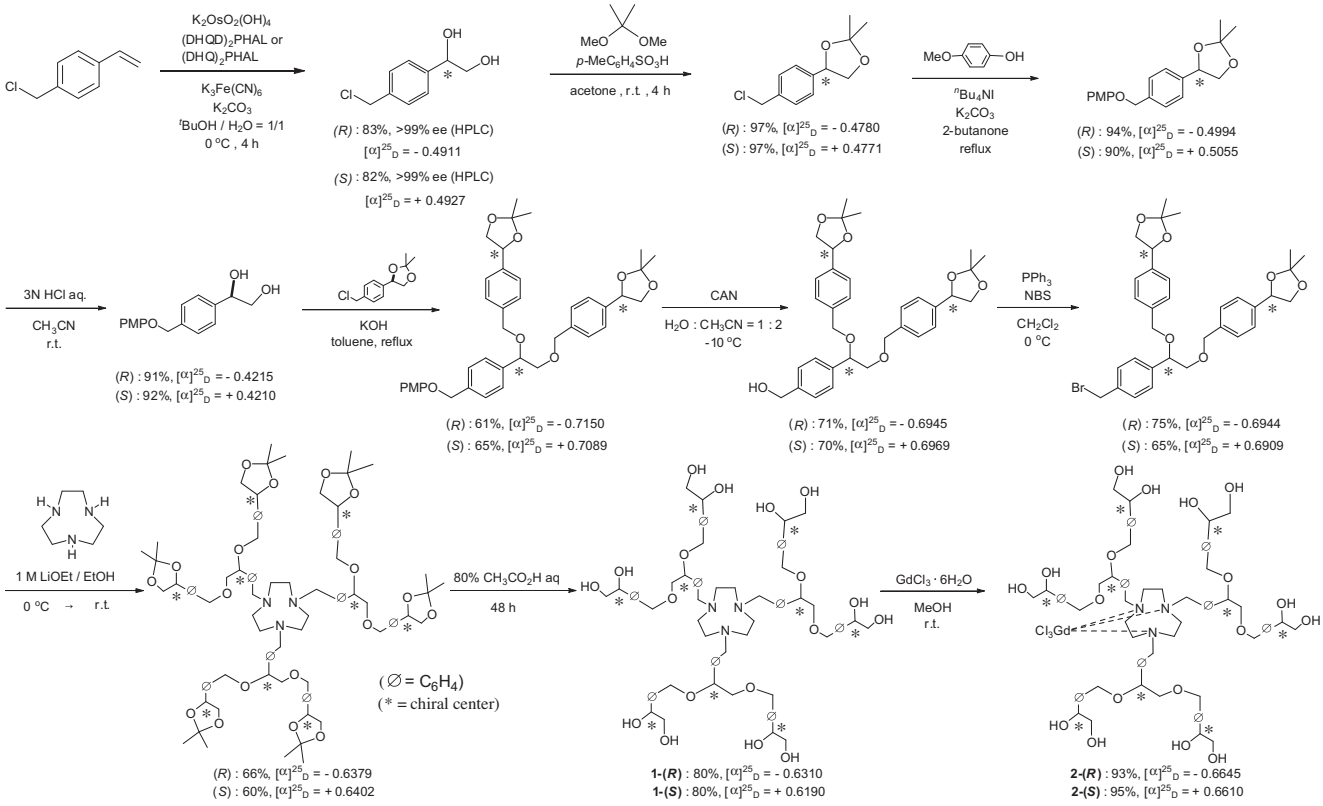

Scheme 1. Synthesis of novel chiral dendrimer–triamine-coordinated Gd complexes, **2-(*R*)** and **2-(*S*)**.

In contrast to amine-terminated dendrimer Gd-MRI contrast agents, such as Gd-functionalized PAMAM and PPI dendrimers, no cytotoxic effect was observed for either **2-(*R*)** or **2-(*S*)** with L929 cells (Fig. 3).[14]

Thus, contrast enhancement by **2-(*R*)** and **2-(*S*)** was evaluated in vivo. Figure 4 shows T1-weighted MR images of mice before and after intravenous injection of **2-(*R*)**, **2-(*S*)**, and Gd-DTPA (0.10 mmol Gd/kg). Since most of the injected Gd-DTPA was excreted through the kidney, and accumulated in the bladder within 30 min, little contrast enhancement was observed except for the kidney. In contrast, no accumulation of **2-(*R*)** or **2-(*S*)** in specific organs, such as the liver and kidney, was observed with high and prolonged contrast enhancement throughout the entire bodies of mice. They also showed improved vascular retention and a moderate renal excretion rate (completely excreted after 24 h).

To accurately discuss the pharmacokinetic differences between optical isomers, the affinities of **2-(*R*)** and **2-(*S*)** with bovine serum albumin (BSA), which is a model of plasma protein, were estimated by a quartz crystal microbalance (QCM) measurement (Fig. 5).[15] As a result, association constant K_a of **2-(*S*)** ($4.02 \times 10^{10}\,M^{-1}$) was about 4 times higher than that of **2-(*R*)** ($9.61 \times 10^{9}\,M^{-1}$), which means that **2-(*S*)** is retained in vasculature for longer after administration in a mouse body. This result was also supported by T1-weighted MR images of mice before and after intravenous injection of **2-(*R*)** and **2-(*S*)** (Fig. 4).

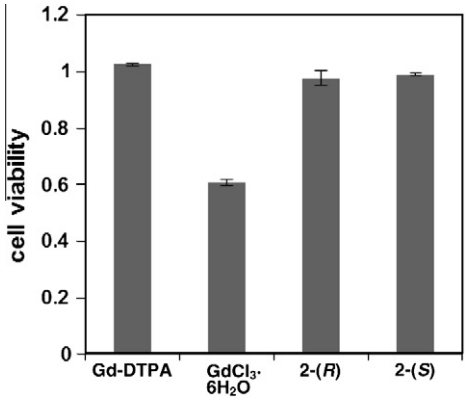

Figure 3. Viabilities of L929 cells exposed Gd-DTPA, $GdCl_3{\cdot}6H_2O$, **2-(*R*)**, and **2-(*S*)** at 0.25 mM.

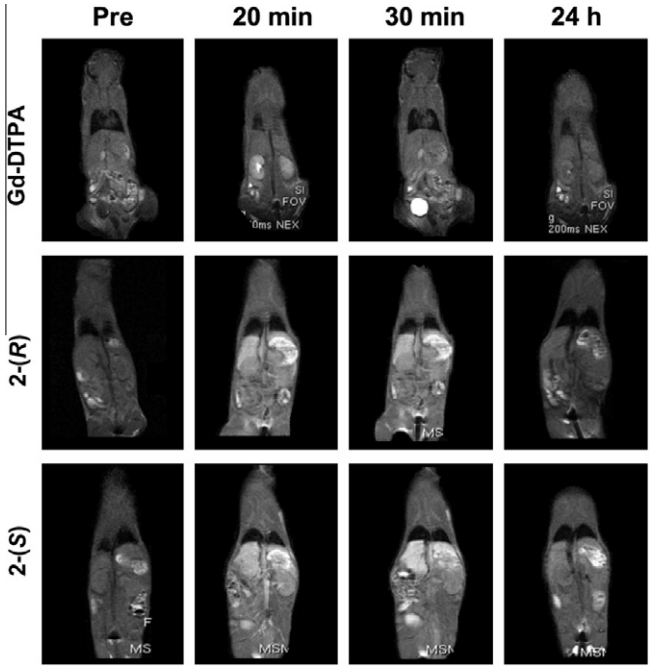

Figure 4. T1-weighted MR images before and after intravenous injection of Gd-DTPA, **2-(*R*)**, and **2-(*S*)**.

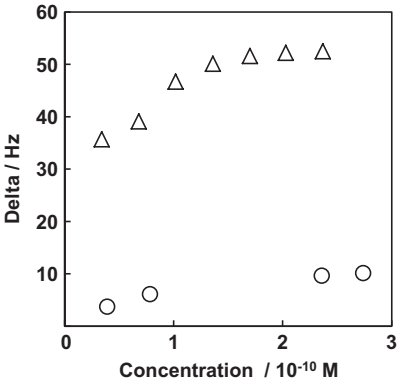

Figure 5. Frequency change of the electrodes coated with BSA after addition of **2-(*R*)** (circular symbol) and **2-(*S*)** (triangular symbol).

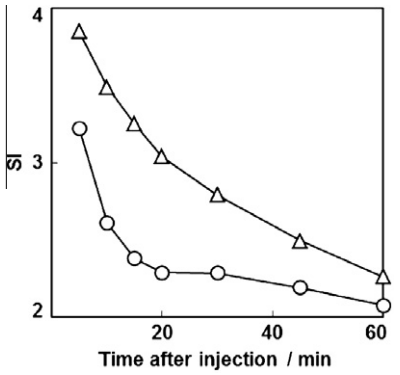

Figure 6. Time-course of the signal intensities (SI) at the blood vessels in MR images after injection of **2-(*R*)** (circular symbol) and **2-(*S*)** (triangular symbol).

More directly, a measurement of the time-course of the signal intensities (SI) at the blood vessels in MR images indicated that the rate of clearance of **2-(*R*)** was faster than that of **2-(*S*)** (Fig. 6). In addition, the concentrations of Gd^{3+} in the blood and urine, 60 min after the injection of **2-(*R*)** and **2-(*S*)**, were quantified by an atomic absorption spectroscopy, which showed that 30.2% of **2-(*R*)** and 20.6% of **2-(*S*)** were transferred to urine, while 22.9% of **2-(*R*)** and 27.8% of **2-(*S*)** were retained in the blood, respectively. All results obtained strongly support that **2-(*S*)** is retained in vasculature for longer than **2-(*R*)** after administration in a mouse body.

Generally, drugs administered in the blood interact with plasma proteins with equilibrium between associated and dissociated states. Upon glomerular filtration, which is an important metabolic pathway, only a chiral contrast agent in the dissociated state can be excreted. Therefore, the difference in the affinities of **2-(*R*)** and **2-(*S*)** for plasma protein might affect their metabolism and result in the difference in their distributions throughout the body.

Conclusions

In conclusion, we have synthesized the first chiral dendrimer–triamine-coordinated Gd contrast agents, and the pharmacokinetic differences between the optical isomers, **2-(*R*)** and **2-(*S*)**, were

clarified. The influence of the dendrimer generations on contrast ability in MRI is now under investigation.

Acknowledgments

This work was partly supported by the Creation of Innovation Centers for Advanced Interdisciplinary Research Areas Program 'Innovative Techno-Hub for Integrated Medical Bio-imaging', and a Grant-in-Aid for the Global COE Program 'Integrated Material Science' from the Ministry of Education, Culture, Sports, Science and Technology (MEXT), Japan. YK acknowledges financial support from Adaptable and Seamless Technology Transfer Program through Target-driven R&D (A-STEP), Japan Science and Technology Agency (JST). TK acknowledges financial support from the Daiwa Securities Health Foundation.

References and notes

1. (a) Bammer, R.; Skare, S.; Newbould, R.; Liu, C.; Thijs, V.; Ropele, S.; Clayton, D. B.; Krueger, G.; Moseley, M. E.; Glover, G. H. *NeuroRx* **2005**, *2*, 167–196.
2. (a) Werner, E. J.; Datta, A.; Jocher, C. J.; Raymond, K. N. *Angew. Chem., Int. Ed.* **2008**, *47*, 8568–8580; (b) Hermann, P.; Kotek, J.; Kubíček, V.; Lukeš, I. *Dalton Trans.* **2008**, 3027–3047; (c) Bottrill, M.; Knok, L.; Long, N. J. *Chem. Soc. Rev.* **2006**, *35*, 557–571; (d) Caravan, P. *Chem. Soc. Rev.* **2006**, *35*, 512–523; (e) Caravan, P.; Ellison, J. J.; McMurry, T. J.; Lauffer, R. B. *Chem. Rev.* **1999**, *99*, 2293–2352.
3. (a) Perazella, M. A. *Clin. J. Am. Soc. Nephrol.* **2009**, *4*, 461–469; (b) Perazella, M. A. *Clin. J. Am. Soc. Nephrol.* **2008**, *3*, 649–651.
4. (a) Villaraza, A. J. L.; Bumb, A.; Brechbiel, M. W. *Chem. Rev.* **2010**, *110*, 2921–2959; Bunb, A.; Brechbiel, M. W.; Choyke, P *Acta Radiol.* **2010**, *51*, 751–767; (c) Langereis, S.; Dirksen, A.; Hackeng, T. M.; van Genderen, M. H. P.; Meijer, E. W. *New J. Chem.* **2007**, *31*, 1152–1160; (d) Kobayashi, H.; Brechbiel, M. W. *Adv. Drug Deliv. Rev.* **2005**, *57*, 2271–2286.
5. (a) Vögtle, F.; Richardt, G.; Werner, N. *Dendrimer Chemistry*; Wiley-VCH: Weinheim, 2009; (b) *Designing Dendrimers*; Campagna, S., Ceroni, P., Puntoriero, F., Eds.; John Wiley & Sons Hoboken: New Jersey, 2012; (c) Astruc, D.; Boisselier, E.; Ornelas, C. *Chem. Rev.* **2010**, *110*, 1857–1959.
6. Wiener, E. C.; Brechbiel, M. W.; Brothers, H.; Magin, R. L.; Gansow, O. A.; Tomalia, D. A.; Lauterbur, P. C. *Magn. Reson. Med.* **1994**, *31*, 1–8; (b) Bryant, L. H., Jr.; Brechbiel, M. W.; Wu, C.; Bulte, J. W. M.; Herynek, V.; Frank, J. A. *J. Magn. Reson. Imaging* **1999**, *9*, 348–352; (c) Labieniec, M.; Watala, C. *Cent. Eur. J. Biol.* **2009**, *4*, 434–451; (d) Kojima, C.; Turkbey, B.; Ogawa, M.; Bernardo, M.; Regino, C. A. S.; Bryant, L. H., Jr.; Choyke, P. L.; Kono, K.; Kobayashi, H. *Nanomedicine* **2011**, *7*, 1001–1008.
7. (a) Kobayashi, H.; Kawamoto, S.; Jo, S.-K.; Bryant, H. L., Jr.; Brechbiel, M. W.; Star, R. A. *Bioconjugate Chem.* **2003**, *14*, 388–394; (b) Langereis, S.; de Lussanet, Q. G.; van Genderen, M. H. P.; Backes, W. H.; Meijer, E. W. *Macromolecules* **2004**, *37*, 3084–3091; (c) KuKowska-Latallo, J. F.; Candido, K. A.; Cao, Z.; Nigavekar, S. S.; Majoros, I. J.; Thomas, T. P.; Balogh, L. P.; Khan, M. K.; Baker, J. R., Jr. *Cancer Res.* **2005**, *65*, 5317–5324.
8. Wiener, E. C.; Auteri, F. P.; Chen, J. W.; Brechbiel, M. W.; Gansow, O. A.; Schneider, D. S.; Belford, R. L.; Clarkson, R. B.; Lauterbur, P. C. *J. Am. Chem. Soc.* **1996**, *118*, 7774–7782.
9. (a) Kolb, H. C.; Sharpless, K. B. In *Transition Metals for Organic Synthesis*; Beller, M., Bolm, C., Eds., 2nd Ed.; Wiley-VCH: Weinheim, 2004; pp 275–298. Vol.2; (b) Kolb, H. C.; VanNieuwenhze, M. S.; Sharpless, K. B. *Chem. Rev.* **1994**, *94*, 2483–2547.
10. Chang, H.-T.; Chen, C.-T.; Kondo, T.; Siuzdak, G.; Sharpless, K. B. *Angew. Chem., Int. Ed. Engl.* **1996**, *35*, 182–186.
11. ***1-(R)***: White powder. ^{1}H NMR ($CDCl_3$, 400 MHz): δ (ppm): 1.98–2.08 (br s, 12H, OH), 2.83 (br s, 12H, $-N(CH_2)_2N-$), 3.49–3.56 (m, 15H), 3.70–4.34 (s, 9H, $-CH(OH)-$), 4.32–4.44 (m, 12H, $-C_6H_4CH_2-$), 4.59–4.64 (m, 9H), 7.16–7.47 (m, 36H, $-C_6H_4-$). ESI TOF MS m/z for $C_{87}H_{105}N_3O_{18}$ $[M+H]^+$: 1480.7858.
1-(S): White powder. ESI TOF MS m/z for $C_{87}H_{105}N_3O_{18}$ $[M+H]^+$: 1480.7228.
Preparation of **2-(*R*)** from the reaction of **1-(*R*)** with $GdCl_3{\cdot}6H_2O$. A solution of $GdCl_3{\cdot}6H_2O$ (46 mg, 125 μmol) in MeOH (1.5 mL) was added dropwise to a solution of **1-(*R*)** (185 mg, 125 μmol) in MeOH (1.0 mL), and the mixture was stirred at room temperature for 24 h. Then, the solvent, MeOH, was removed under vacuum to give **2-(*R*)** (202 mg, 116 μmol, 93%) as a white powder. **2-(*R*)**: MALDI TOF MS (matrix: DCTB) m/z for $C_{87}H_{105}ClGdN_3O_{18}$ [M-2Cl]+: 1669.6334 (7%), 1670.6258 (46%), 1671.6252 (75%), 1672.6242 (100%), 1673.6264 (80%), 1674.6282 (84%), 1675.6292 (54%), 1676.6334 (25%), 1677.6376 (3%), 1678.6410 (2%). The same procedure gave **2-(*S*)** in 95% yield. **2-(*S*)**: White powder. ESI-TOF MS m/z for $C_{87}H_{105}Cl_3GdN_3O_{18}$ [M]+: 1741.5671 (13%), 1742.5467 (40%), 1743.5668 (100%), 1744.5619 (60%), 1745.5624 (19%), 1746.2629 (14%), 1747.5433 (18%).
12. The increase in the coordination number of free water to the present novel MRI contrast agents, **2-(*R*)** and **2-(*S*)**, was shown by preliminary XAFS measurements using the SPring 8 synchrotron radiation facility.
13. The strong binding (coordination) ability of 1,4,7-triazacyclononanes as ligands to transition-metals was shown in the stability of 1,4,7-triazacyclononane-coordinated Fe, Cu, Ru, and Rh complexes under both acidic and basic conditions. For Fe: (a) Dorazio, S. J.; Tsitovich, P. B.; Siters, K. E.; Spernyak, J. A.; Morrow, J. R. *J. Am. Chem. Soc.* **2011**, *133*, 14154–14156; For Cu and Ru: (b) Medvetz, D. A.; Stakleff, K. D.; Schreiber, T.; Custer, P. D.; Hindi, K.; Panzner, M. J.; Blanco, D. D.; Taschner, M. J.; Tessier, C. A.; Youngs, W. J. *J. Med. Chem.* **2007**, *50*, 1703–1706; (c) Chan, S. L.-F.; Kan, Y.-H.; Yip, K.-L.; Huang, J.-S.; Che, C.-M. *Coord. Chem. Rev.* **2011**, *255*, 899–919. For Rh:; (d) Zhou, R.; Wang, Y.; Hu, Y.; Flood, T. C. *Organometallics* **1997**, *16*, 434–441.
14. Malic, N.; Wiwattanapatapee, R.; Klopsch, R.; Lorenz, K.; Frey, H.; Weener, J. W.; Meijer, E. W.; Paulus, W.; Duncan, R. *J. Control. Release* **2000**, *65*, 133-148.
*Cytotoxicity examination of **2-(R)** and **2-(S)**.* L929 mouse fibroblasts were plated into each well of 96-multiwell cell culture plates at a density of 1×10^4 cells/cm^2. The culture medium (D-MEM/F-12 with 10% FBS, 100 U/mL penicillin and 100 μg/mL streptomycin) was changed to the fresh medium containing 0.25 mM of the chemicals 24 h after cell seeding. Followed the incubation for 48 h at 37 °C under 5% CO_2 −95 % air atmosphere, the culture medium was replaced to the fresh medium (100 μL) containing Cell Count Reagent SF (Nacalai Tesque Inc., Kyoto, Japan; 10 μL), and plates were incubated for 3 h at 37 °C. Then, the absorbance at 450 nm was measured by the spectrophotometer (VersaMax, Molecular Devices Inc., Union City, CA). The absorbance was normalized by that of cells proliferated with the culture medium without the chemicals.
15. G.G. Guilbault, *Applications of Piezoelectric Quartz Crystal Microbalances*, C. Lu, A.W. Czanderna (Eds.), Elsevier, New York, 1984, pp. 251-280.
*Binding ability examination of **2-(R)** and **2-(S)** with BSA by a quartz crystal microbalance (QCM) measurement.* Binding ability of **2-(*R*)** or **2-(*S*)** to BSA was evaluated through Affinix-Q® system (Initium Inc., Tokyo, Japan) according to the procedure instructed from manufacturer. Briefly, the quartz crystal adsorbed BSA physically (ca. 0.19 fmol) was placed into 500 μL of solutions with various concentrations of **2-(*R*)** or **2-(*S*)**. Following the diagrammatic representation of frequency change of the crystal against the concentration of **2-(*R*)** or **2-(*S*)**, the dissociation rate constant (K_d) was estimated by non-linear regression fitting of the saturated adsorption amount at each concentration, and the association rate constant (K_a) was calculated as $1/K_d$.